



Kinetics of dimethyl sulfide (DMS) reactions with isoprene-derived Criegee intermediates studied with direct UV absorption

Mei-Tsan Kuo¹, Isabelle Weber², Christa Fittschen², Jim Jr-Min Lin^{1,3}

¹Institute of Atomic and Molecular Sciences, Academia Sinica, Taipei 10617, Taiwan

²Univ. Lille, CNRS, UMR 8522 - PC2A - Physicochimie des Processus de Combustion et de l'Atmosphère, F-59000 Lille, France

³Department of Chemistry, National Taiwan University, Taipei 10617, Taiwan

Correspondence to: Jim Jr-Min Lin (jimlin@gate.sinica.edu.tw)

Abstract. Criegee intermediates (CIs) are formed in the ozonolysis of unsaturated hydrocarbons and play a role in atmospheric chemistry as a non-photolytic OH source or a strong oxidant. Using a relative rate method in an ozonolysis experiment, Newland et al. [Atmos. Chem. Phys., 15, 9521-9536, 2015] reported high reactivity of isoprene-derived Criegee intermediates towards dimethyl sulfide (DMS) relative to that towards SO₂ with the ratio of the rate coefficients $k_{\text{DMS+CI}} / k_{\text{SO}_2+\text{CI}} = 3.5 \pm 1.8$. Here we reinvestigated the kinetics of DMS reactions with two major Criegee intermediates formed in isoprene ozonolysis, CH₂OO and methyl vinyl ketone oxide (MVKO). The individual CI was prepared following reported photolytic method with suitable (diiodo) precursors in the presence of O₂. The concentration of CH₂OO or MVKO was monitored directly in real time through their intense UV-visible absorption. Our results indicate the reactions of DMS with CH₂OO and MVKO are both very slow; the upper limits of the rate coefficients are 4 orders of magnitude smaller than that reported by Newland et al. These results suggest that the ozonolysis experiment could be complicated such that interpretation should be careful and these CIs would not oxidize atmospheric DMS at any substantial level.

1 Introduction

As a non-photolytic OH source or a strong oxidant, Criegee intermediates (CIs) influence the chemical processes in the troposphere (Nguyen et al., 2016; Novelli et al., 2014; Johnson and Marston, 2008; Atkinson and Aschmann, 1993; Gutbrod et al., 1997; Zhang et al., 2002) and, ultimately, have impact on the formation of secondary aerosols and other pollutants (Percival et al., 2013; Wang et al., 2016; Meidan et al., 2019). A detailed understanding of CI chemistry under atmospheric conditions is, thus, necessary to be able to accurately predict and describe the evolution of Earth's atmosphere.

However, due to their high reactivity and, hence, short lifetimes, laboratory studies of the reactions of CIs have been challenging. In fact, no direct detection of CIs has been known before Welz et al. reported a novel method to efficiently generate CIs other than through ozonolysis of alkenes (Welz et al., 2012). They utilized (R1) and (R2) to prepare CH₂OO and directly measured the rate coefficients of CH₂OO reactions with SO₂ and NO₂ by following the time-resolved decay of CH₂OO.



Surprisingly, the obtained rate coefficients are up to 10^4 times larger than previous results deduced from ozonolysis experiments, indicating that the ozonolysis experiments could be quite complicated such that reliable kinetic results may be
 35 hard to retrieve.

After this pioneering work, the same method has been applied for generation of other CIs, like CH_3CHOO (Taatjes et al., 2013), $(\text{CH}_3)_2\text{COO}$ (Liu et al., 2014a) and methyl vinyl ketone oxide (MVKO) (Barber et al., 2018), methacrolein oxide (MACRO) (Vansco et al., 2019), etc. These CIs have been identified with various detection methods, like photoionization mass spectrometry (Taatjes et al., 2013), infrared action (Liu et al., 2014b) and absorption (Su et al., 2013; Lin et al., 2015)
 40 spectroscopy, UV-visible spectroscopy (Beames et al., 2013; Sheps, 2013; Liu et al., 2014a; Ting et al., 2014; Smith et al., 2014; Chang et al., 2016), microwave spectroscopy (McCarthy et al., 2013; Nakajima et al., 2015), etc. In addition, utilizing the direct detection of CIs, a number of kinetic investigations of CI reactions, e.g., with SO_2 (Huang et al., 2015), water vapor (Chao et al., 2015), alcohols (Chao et al., 2019), thiols (Li et al., 2019), amines (Chhantyal-Pun et al., 2019), carbonyl molecules (Taatjes et al., 2012), and organic (Welz et al., 2014) and inorganic (Foreman et al., 2016) acids, etc., have been
 45 reported (Lee, 2015; Osborn and Taatjes, 2015; Lin and Chao, 2017; Khan et al., 2018).

Recently, Newland et al. studied the reactivity of CIs with H_2O and, for the first time, with dimethyl sulfide (DMS) in the ozonolysis of isoprene at the EUPHORE simulation chamber facility and found a rapid reaction of CIs with DMS (Newland et al., 2015). A mixture of CH_2OO , MVKO and MACRO was generated through ozonolysis of isoprene with a total CI yield of 0.57 (Newland et al., 2015). The yields of the individual CIs have previously been estimated to be 0.31 for CH_2OO , 0.21
 50 for MVKO, and 0.05 for MACRO (Zhang et al., 2002; Nguyen et al., 2016). To determine reaction rates, Newland et al. used a relative rate method and followed the removal of SO_2 versus the removal of other reactants. For the reaction $\text{CI} + \text{DMS}$ relative to the reaction $\text{CI} + \text{SO}_2$, they obtained a relative rate coefficient of $k_{\text{DMS}+\text{CI}} / k_{\text{SO}_2+\text{CI}} = 3.5 \pm 1.8$ (Newland et al., 2015). Since the reactions of typical CIs with SO_2 are very fast, with rate coefficients on the order of $4 \times 10^{-11} \text{ cm}^3 \text{ s}^{-1}$ (Welz et al., 2012; Lee, 2015; Osborn and Taatjes, 2015; Lin and Chao, 2017; Khan et al., 2018), this result suggests that the reaction
 55 of $\text{CI} + \text{DMS}$ is extremely fast, with a rate coefficient of ca. $10^{-10} \text{ cm}^3 \text{ s}^{-1}$. This value is extremely large, close to those of the fastest reactions of CIs.

Newland et al. noted, however, that the presented rate coefficients do not correspond to the rates of single elementary reactions but rather describe the general reactivity of CIs towards DMS or H_2O under conditions similar to the atmospheric boundary layer (Newland et al., 2015).

60 DMS is the major sulfur containing species in the atmosphere with high abundances in the marine boundary layer (Yvon et al., 1996) but also e.g. in the Amazon basin (Jardine et al., 2015), and has been shown to play an important role in the formation of SO_2 and sulfuric acid, which are precursors of sulfide aerosols (Andreae and Crutzen, 1997; Charlson et al., 1987; Faloona, 2009). The results of Newland et al. (Newland et al., 2015) therefore suggest that in regions with high concentrations of CIs, the $\text{CI} + \text{DMS}$ reactions will have a comparable impact on the oxidation of DMS, considering the



65 main atmospheric oxidants are OH and NO₃ ($k_{\text{DMS}+\text{OH}} = 4.8 \times 10^{-12} \text{ cm}^3 \text{ s}^{-1}$, $k_{\text{DMS}+\text{NO}_3} = 1.1 \times 10^{-12} \text{ cm}^3 \text{ s}^{-1}$ (Atkinson et al., 2004)).

Here we report the first direct kinetic study of the reactions of CH₂OO and MVKO, the main CIs formed in the ozonolysis of isoprene with DMS. CIs have strong UV-visible absorption (Lin and Chao, 2017). For example, CH₂OO and MVKO absorb strongly (peak cross section $\sigma \geq 1 \times 10^{-17} \text{ cm}^2$) in the wavelength ranges of 285–400 nm (Ting et al., 2014; Lewis et al., 2015) and 315–425 nm (Vansco et al., 2018; Caravan et al., 2020) (> 20% of the peak value), respectively. This strong and distinctive absorption has been utilized to probe CIs in a number of kinetic experiments, including their reactions with SO₂, water vapor, alcohols, thiols, organic and inorganic acids, carbonyl compounds, alkenes, etc. (Khan et al., 2018; Lin and Chao, 2017; Osborn and Taatjes, 2015; Lee, 2015). In this work, both CH₂OO and MVKO were directly probed in real time via their strong UV absorption at 340 nm.

75 Surprisingly, our experimental results do not indicate any significant reactivity of DMS with CH₂OO or MVKO. We therefore propose upper limits of the rate coefficients for these reactions. Implications for atmospheric chemistry are discussed.

2 Experimental setup

The experimental setup has been described previously (Chao et al., 2015; Chao et al., 2019). To generate CH₂OO and MVKO, we followed the approaches of Welz et al. (Welz et al., 2012) and Barber et al., respectively. The MVKO formation is through the reaction sequence $\text{ICH}_2\text{-CH=C(I)-CH}_3 + h\nu \rightarrow \text{CH}_3(\text{C}_2\text{H}_3)\text{CI} + \text{I}$, $\text{CH}_3(\text{C}_2\text{H}_3)\text{CI} + \text{O}_2 \rightarrow \text{MVKO} + \text{I}$, analogue to reactions (R1) and (R2) (Barber et al., 2018). Note that because the MVKO precursor (ICH₂-CH=C(I)-CH₃, 1,3-diiodo-2-butene) does not absorb light at 308 nm (XeCl excimer laser), we used a photolysis laser at 248 nm (KrF excimer laser) for generating MVKO. However, DMS absorbs weakly at 248 nm. We therefore performed additional experiments by photolyzing CH₂I₂ at 248 nm to assess the impact of DMS photolysis at 248 nm on the decay of the CIs.

Experiments were conducted in a photolysis reactor (inner diameter: 1.9 cm, effective length: 71 cm). The photolysis laser beam was coupled into and out of the reactor by two long-pass filters (248 nm: Eksma Optics, custom-made 275 nm long-pass; 308 nm: Semrock LP03-325RE-25) and monitored with an energy meter (Gentec EO, QE25SP-H-MB-D0). The probe light was from a plasma Xe lamp (Energetiq, EQ-99) (Su and Lin, 2013) and directed through the reactor collinearly with the photolysis beam. It passes through the reactor six times, resulting in an effective absorption path length of ca. 426 cm. After passing through band-pass filters (340 nm, Edmund, #65129, 10 nm bandwidth, OD 4), the probe beam and a reference beam which did not pass through the reactor were both focused on a balanced photodiode detector (Thorlabs, PDB450A). Output signals were recorded in real time with a high-resolution oscilloscope (LeCroy, HDO4034, 4096 vertical resolution) and averaged for 120 laser shots (repetition rate ~1 Hz). We observed a small time-dependent variation in transmittance even when no precursor was introduced into the reactor. To compensate for this effect, which was caused by



the optics and the photolysis laser pulse, we recorded background traces without adding the precursor before and after each set of experiments. The reported data are after background subtraction.

All reactant gas flows were controlled by calibrated mass-flow controllers (Brooks: 5850E, 5800E and Bronkhorst: EL-FLOW prestige) and mixed before entering the reactor. Reactant concentrations were determined prior to mixing of the reactant flows by UV absorption spectroscopy in two separate absorption cells for either DMS (absorption path length 90.4 cm for $[DMS] \leq 1.7 \times 10^{15} \text{ cm}^{-3}$ or 20.1 cm for $[DMS] \leq 8.1 \times 10^{15} \text{ cm}^{-3}$) or the respective diiodo precursors (absorption path length 90.4 cm) using the reported absorption cross sections (Sander et al., 2011; Limão-Vieira et al., 2002). However, because no absorption cross sections for 1,3-diiodo-2-butene have been reported, its absolute concentration cannot be determined. Typical concentration ranges were: $[CH_2I_2] = (0.23\text{--}2.54) \times 10^{14} \text{ cm}^{-3}$, $[O_2] = (3.28\text{--}3.30) \times 10^{17} \text{ cm}^{-3}$, and $[DMS] = (0\text{--}8.1) \times 10^{15} \text{ cm}^{-3}$. We assume ideal gas behavior for the concentration calculation. The majority of the experiments were performed at 300 Torr (N_2) and 298 K.

3 Results and discussion

3.1. $CH_2OO + DMS$

Representative time traces of CH_2OO absorption recorded at $340 \pm 5 \text{ nm}$ ($\sigma = 1.23 \times 10^{-17} \text{ cm}^2$ at 340 nm) (Ammann et al., 2015; Ting et al., 2014) under various $[DMS]$ are depicted in Fig. 1. Similar results but recorded with different initial concentrations of CH_2I_2 and/or different photolysis laser fluences are displayed in Figs. S11–S13. At $t = 0$, CH_2OO is generated within 10^{-5} s by photolysis of CH_2I_2 at 308 nm (nanosecond pulsed laser) (R1) and the fast reaction of CH_2I with O_2 (R2) ($k_{O_2} = 1.4 \times 10^{-12} \text{ cm}^3 \text{ s}^{-1}$ (Eskola et al., 2006); $[O_2] = 3.3 \times 10^{17} \text{ cm}^{-3}$). The subsequent decay in absorption is due to the consumption of CH_2OO either through reaction with DMS or through other reaction processes, e.g., bimolecular reactions with radical byproducts like I atoms, wall loss, etc. We can see that the decay curves of CH_2OO at various $[DMS]$ are extremely similar to one another, indicating that the reaction of $CH_2OO + DMS$ is not significant.

The decay of CH_2OO can be well described with an exponential function ($R^2 > 0.995$) (e.g., Fig. 1).

$$[CH_2OO](t) = [CH_2OO]_0 e^{-k_{obs}t} \quad (1)$$

The fitting error of k_{obs} is less than 1% mostly. Under the conditions of this study, the consumption of CH_2OO can be described as

$$-\frac{d[CH_2OO]}{dt} = k_{obs}[CH_2OO] = (k_0 + k_{DMS+CH_2OO}[DMS])[CH_2OO] \quad (2)$$

where k_0 represents the sum of the effective rate coefficients for all consumption channels of CH_2OO except its reaction with DMS, which is described as the bimolecular rate coefficient k_{DMS+CH_2OO} .

The CH_2OO decay rate coefficients k_{obs} as functions of $[DMS]$ for different photolysis laser fluences are summarized in Fig. 2. At higher laser fluences, more CH_2OO and radical byproducts are generated, resulting in shorter CH_2OO lifetimes (see Fig. S7: plot of k_0 against $[CH_2I_2] \times I_{308nm}$), similar to previous works (Smith et al., 2016; Li et al., 2020; Zhou et al.,



2019). The slopes of the linear fits of Fig. 2 would correspond to $k_{\text{DMS}+\text{CH}_2\text{OO}}$ (see Eq. (2)). However, the slope values are quite small, close to our detection limit (Lin et al., 2018). Within experimental uncertainty, $k_{\text{DMS}+\text{CH}_2\text{OO}}$ exhibits no clear correlation to the photolysis laser fluence and other experimental conditions like $[\text{CH}_2\text{I}_2]$ (see Table S1 and Fig. S9). From a total of 11 experimental data sets (Exp#1–11, Table S1), we inferred an average $k_{\text{DMS}+\text{CH}_2\text{OO}} = (1.2 \pm 1.0) \times 10^{-15} \text{ cm}^3 \text{ s}^{-1}$ (error bar is one standard deviation of the 11 data points).

3.2. Test of the effect of DMS photolysis

Although the absorption cross section of DMS is quite small ($1.28 \times 10^{-20} \text{ cm}^2$ at 248 nm and $< 1 \times 10^{-22} \text{ cm}^2$ at 308 nm) (Hearn et al., 1990), yet the photolysis of DMS, especially at 248 nm, should be considered. We have performed a quantitative estimation of radical concentrations originating from the photolysis of DMS under the experimental conditions of this work (page S7) and show the results in Table S4.

In order to reduce the influence of DMS photolysis for the MVKO experiments, which require 248 nm photolysis (see Sect. 3.3), we constraint $[\text{DMS}] \leq 1.7 \times 10^{15} \text{ cm}^{-3}$ and the laser fluence $I_{248\text{nm}} \leq 3.72 \text{ mJ cm}^{-2}$. Then the amount of dissociated $[\text{DMS}]$ would be $\leq 1 \times 10^{11} \text{ cm}^{-3}$, smaller than the dissociated $[\text{CH}_2\text{I}_2] \cong 1.2 \times 10^{12} \text{ cm}^{-3}$ by an order of magnitude or more.

The expected products of DMS photolysis are $\text{CH}_3 + \text{CH}_3\text{S}$ (Bain et al., 2018), which are less reactive than I atoms or CIs. Thus, the small amount of dissociated $[\text{DMS}]$ would only have a minor effect. And indeed, the results of $\text{CH}_2\text{OO}+\text{DMS}$ reaction obtained with 248 nm photolysis (Figs. S2, S14, Table S2) are very similar to those with 308 nm photolysis (Figs. 2, S1, S11–S13, Table S1), indicating the effect of DMS photolysis is very minor. The values of $k_{\text{DMS}+\text{CH}_2\text{OO}}$ obtained with 248 nm photolysis (Table S2) range from 1.6×10^{-15} to $3.2 \times 10^{-15} \text{ cm}^3 \text{ s}^{-1}$, which are only slightly higher than the results obtained with 308 nm photolysis (see Fig. S9). This indicates that the effect of the DMS photolysis would be on the order of $(1-3) \times 10^{-15} \text{ cm}^3 \text{ s}^{-1}$ for $k_{\text{DMS}+\text{CH}_2\text{OO}}$.

3.3. MVKO + DMS

Typical absorbance-time profiles of MVKO under various $[\text{DMS}]$ ($\leq 1.3 \times 10^{15} \text{ cm}^{-3}$) are presented in Fig. 3. When generating MVKO via the reaction of $\text{CH}_3(\text{C}_2\text{H}_3)\text{CI} + \text{O}_2$ at a high pressure like 300 Torr, the MVKO signal profiles rise slower than those of CH_2OO , with the maximum of the MVKO signal being at about 1.5 ms. Based on detailed kinetic and quantum chemical results, which will be published elsewhere, we have concluded that the slow rise of the MVKO signal is due to the thermal decomposition of an adduct, $\text{CH}_3(\text{C}_2\text{H}_3)\text{CIOO} \rightarrow \text{CH}_3(\text{C}_2\text{H}_3)\text{COO} + \text{I}$ (Lin et al., 2020). See SI (Sect. S3, page S5) for details. This difference is consistent with the fact that MVKO is resonance-stabilized due to the extended conjugation of its vinyl group (Barber et al., 2018) and thus the adduct $\text{CH}_3(\text{C}_2\text{H}_3)\text{CIOO}$ is relatively less stable due to disruption of the conjugation. Nevertheless, no significant changes in the absorbance-time profiles of MVKO with varying $[\text{DMS}]$ can be noted (Fig. 3 inset), indicating the reaction of $\text{MVKO}+\text{DMS}$ is insignificant. In Fig. 3, we can see that the lifetime of MVKO is on the order of 10 ms (i.e., a decay rate coefficient of ca. 100 s^{-1}) and the variation of the MVKO



signal is insignificant upon adding [DMS]. This indicates that the reaction with DMS only changes, at the most, the MVKO lifetime by a small fraction (< 0.1) (a larger change would cause obvious deviation from the experimental observations of Fig. 3). Thus, $k_{\text{DMS+MVKO}}$ can be estimated to be on the order of $(100 \text{ s}^{-1})(0.1)/(1.3 \times 10^{15} \text{ cm}^{-3}) \cong 10^{-14} \text{ cm}^3 \text{ s}^{-1}$. Similar conclusion can be drawn from additional profiles recorded with different precursor concentrations and photolysis laser fluences or at different pressures (Fig. S15–S17).

To obtain more quantitative values of $k_{\text{DMS+MVKO}}$, we performed kinetic analysis and the details are given in SI (Sect. S3); selected results of k_{obs} as functions of [DMS] are presented in Fig. 4. Similar to the $\text{CH}_2\text{OO} + \text{DMS}$ case, the rate coefficients for the reaction $\text{MVKO} + \text{DMS}$ show no clear dependence on laser fluence and precursor concentration. From a total of 15 experiment sets (Exp#15–29, Table S3), we obtain an average rate coefficient $k_{\text{DMS+MVKO}} = (6.2 \pm 3.3) \times 10^{-15} \text{ cm}^3 \text{ s}^{-1}$ (error bar is one standard deviation of the 15 data points). As mentioned above, the MVKO precursor does not absorb light at 308 nm and requires 248 nm photolysis, such that small amounts of DMS would also be photodissociated. However, the above $\text{CH}_2\text{OO} + \text{DMS}$ results indicate that the effect of DMS photolysis in our experiments is minor (on the order of $(1-3) \times 10^{-15} \text{ cm}^3 \text{ s}^{-1}$ for $k_{\text{DMS+CH}_2\text{OO}}$), but may still lead to overestimation of $k_{\text{DMS+MVKO}}$. In this regard, the true value of $k_{\text{DMS+MVKO}}$ may be smaller than the above number.

3.4 Upper limiting rate coefficients and implications for atmospheric modelling

The experimental values of $k_{\text{DMS+CI}}$ (Tables S1 and S3) are quite small, and their standard deviations are comparable to their average values, indicating that the measured $k_{\text{DMS+CI}}$ are close to our detection limit. Here we choose the boundary of three standard deviations as the upper limits for $k_{\text{DMS+CI}}$, $k_{\text{DMS+CH}_2\text{OO}} \leq 4.2 \times 10^{-15} \text{ cm}^3 \text{ s}^{-1}$ and $k_{\text{DMS+MVKO}} \leq 1.6 \times 10^{-14} \text{ cm}^3 \text{ s}^{-1}$ (Table 1). From Table 1, we can see that for the reactions of both CIs studied, the upper limits of the rate coefficients for their reactions with DMS, k_{DMS} , are much smaller than the literature values of their reactions with SO_2 , k_{SO_2} . The resulting ratios $k_{\text{DMS}}/k_{\text{SO}_2}$ are about four orders of magnitude smaller than that reported by Newland et al. (Newland et al., 2015)

The steady-state concentrations of CIs, $[\text{CI}]_{\text{ss}}$, in the troposphere have not been well established yet (Kim et al., 2015; Khan et al., 2018; Vereecken et al., 2017; Bonn et al., 2014; Boy et al., 2013). Novelli et al. have estimated an average CI concentration of $5 \times 10^4 \text{ molecules cm}^{-3}$ (with an order of magnitude uncertainty) for two environments they have investigated (Novelli et al., 2017). Due to fast thermal decomposition (Li et al., 2020; Smith et al., 2016; Vereecken et al., 2017; Stephenson and Lester, 2020) and/or fast reaction with water vapor (Chao et al., 2015; Lee, 2015; Osborn and Taatjes, 2015; Lin and Chao, 2017; Khan et al., 2018), $[\text{CI}]_{\text{ss}}$ is expected to be low, at least a couple of orders of magnitude lower than the steady-state $[\text{OH}]_{\text{ss}}$. The small k_{DMS} values obtained in this work imply that these reactions would not compete with the conventional DMS oxidation pathways like the reactions with OH or NO_3 , of which both the reactant concentrations and rate coefficients are significantly larger.

Newland et al. performed their experiments on a mixture of 3 CIs (CH_2OO , MVKO, MACRO) as resulting from the ozonolysis of isoprene (Newland et al., 2015). The presence of these 3 CIs, however, cannot explain the four orders of



190 magnitude difference to our results. Due to the low yield of MACRO (0.05) compared to the yield of 0.5 for $\text{CH}_2\text{OO} + \text{MVKO}$ (Zhang et al., 2002), it would require an unreasonably large $k_{\text{DMS}+\text{MACRO}}$ in the order of $10^{-9} \text{ cm}^3 \text{ s}^{-1}$, to explain the conclusion of Newland et al.

For the determination of the relative rate of the $\text{Cl} + \text{DMS}$ reaction, Newland et al. monitored the consumption of SO_2 over a measurement period of up to 60 min until approximately 25% of isoprene was consumed (Newland et al., 2015).
195 Additional uncharacterized sources and/or sinks of SO_2 and DMS would lead to a bias in the inferred rate coefficients. A more likely cause for the discrepancies is differences in chemical compositions of the studied reaction mixtures and, hence, the different impact of side reactions. While our direct measurements and kinetics are very straightforward, the ozonolysis experiments of Newland *et al.* might have been more complex than the authors (Newland et al., 2015) had assumed. For example, one may consider the possibility of converting DMS to SO_2 via surface or gas-phase reactions (Chen et al., 2018)
200 under the complicated conditions of isoprene ozonolysis.

4 Summary

In this work, we present the first direct kinetic study of the reactions of DMS with CH_2OO and MVKO , which are the major CIs formed in the ozonolysis of isoprene. We generate the individual CIs by photolysis of the corresponding diiodo precursors in the presence of O_2 and monitored their decay via their strong UV absorption at 340 nm in real time. Our results
205 do not indicate any notable reactivity of DMS with the two CIs studied. We therefore inferred the rate coefficients $k_{\text{DMS}+\text{CH}_2\text{OO}} \leq 4.2 \times 10^{-15} \text{ cm}^3 \text{ s}^{-1}$ and $k_{\text{DMS}+\text{MVKO}} \leq 1.6 \times 10^{-14} \text{ cm}^3 \text{ s}^{-1}$. Our results indicate that even in regions with high abundance of CIs and high concentrations of DMS, the isoprene-derived CIs will not notably contribute to the oxidation of DMS.

Acknowledgements

210 This work is supported by Academia Sinica and Ministry of Science and Technology, Taiwan (MOST 106-2113-M-001-026-MY3; 108-2911-I-001-501(Orchid project)) and French Ministry of Europe and Foreign Affairs through the PHC Orchid project no. 40930 YC.

References

Andreae, M. O., and Crutzen, P. J.: Atmospheric aerosols: biogeochemical sources and role in atmospheric chemistry,
215 Science, 276, 1052-1058, <https://doi.org/10.1126/science.276.5315.1052>, 1997.



- Ammann, M., Cox, R. A., Crowley, J. N., Herrmann, H., Jenkin, E., McNeill, V. F., Mellouki, A., Troe, M. J., and Wallington, T. J.: Task Group on Atmospheric Chemical Kinetic Data Evaluation – Evaluated Kinetic Data (IUPAC 2015 recommendation), <http://iupac.pole-ether.fr>, 2015.
- Atkinson, R., and Aschmann, S. M.: Hydroxyl radical production from the gas-phase reactions of ozone with a series of alkenes under atmospheric conditions, *Environ. Sci. Technol.*, 27, 1357-1363, <https://doi.org/10.1021/es00044a010>, 1993.
- Atkinson, R., Baulch, D. L., Cox, R. A., Crowley, J. N., Hampson, R. F., Hynes, R. G., Jenkin, M. E., Rossi, M. J., and Troe, J.: Evaluated kinetic and photochemical data for atmospheric chemistry: Volume I - gas phase reactions of Ox, HOx, NOx and SOx species, *Atmos. Chem. Phys.*, 4, 1461-1738, <https://doi.org/10.5194/acp-4-1461-2004>, 2004.
- Atkinson, R., Baulch, D. L., Cox, R. A., Crowley, J. N., Hampson, R. F., Hynes, R. G., Jenkin, M. E., Rossi, M. J., Troe, J., and Wallington, T. J.: Evaluated kinetic and photochemical data for atmospheric chemistry: Volume IV – gas phase reactions of organic halogen species, *Atmos. Chem. Phys.*, 8, 4141-4496, <https://doi.org/10.5194/acp-8-4141-2008>, 2008.
- Bain, M., Hansen, C. S., and Ashfold, M. N. R.: Communication: Multi-mass velocity map imaging study of the ultraviolet photodissociation of dimethyl sulfide using single photon ionization and a PImMS2 sensor, *J. Chem. Phys.*, 149, 081103, <https://doi.org/10.1063/1.5048838>, 2018.
- Barber, V. P., Pandit, S., Green, A. M., Trongsiwat, N., Walsh, P. J., Klippenstein, S. J., and Lester, M. I.: Four-carbon Criegee intermediate from isoprene ozonolysis: methyl vinyl ketone oxide synthesis, infrared spectrum, and OH production, *J. Am. Chem. Soc.*, 140, 10866-10880, <https://doi.org/10.1021/jacs.8b06010>, 2018.
- Beames, J. M., Liu, F., Lu, L., and Lester, M. I.: UV spectroscopic characterization of an alkyl substituted Criegee intermediate CH_3CHOO , *J. Chem. Phys.*, 138, 244307, <https://doi.org/10.1063/1.4810865>, 2013.
- Bonn, B., Bourtsoukidis, E., Sun, T. S., Bingemer, H., Rondo, L., Javed, U., Li, J., Axinte, R., Li, X., Brauers, T., Sonderfeld, H., Koppmann, R., Sogachev, A., Jacobi, S., and Spracklen, D. V.: The link between atmospheric radicals and newly formed particles at a spruce forest site in Germany, *Atmos. Chem. Phys.*, 14, 10823-10843, <https://doi.org/10.5194/acp-14-10823-2014W>, 2014.
- Boy, M., Mogensen, D., Smolander, S., Zhou, L., Nieminen, T., Paasonen, P., Plass-Dülmer, C., Sipilä, M., Petäjä, T., Mauldin, L., Berresheim, H., and Kulmala, M.: Oxidation of SO_2 by stabilized Criegee intermediate (sCI) radicals as a crucial source for atmospheric sulfuric acid concentrations, *Atmos. Chem. Phys.*, 13, 3865-3879, <https://doi.org/10.5194/acp-13-3865-2013>, 2013.
- Caravan, R. L., Vansco, M. F., Au, K., Khan, M. A. H., Li, Y.-L., Winiberg, F. A. F., Zuraski, K., Lin, Y.-H., Chao, W., Trongsiwat, N., Walsh, P. J., Osborn, D. L., Percival, C. J., Lin, J. J.-M., Shallcross, D. E., Sheps, L., Klippenstein, S. J., Taatjes, C. A., and Lester, M. I.: First direct kinetic measurements and theoretical predictions of an isoprene-derived Criegee intermediate with implications for aerosol formation, *Proc. Natl. Acad. Sci., PNAS Latest Articles*, <https://doi.org/10.1073/pnas.1916711117>, 2020.
- Chang, Y.-P., Chang, C.-H., Takahashi, K., and Lin, J. J.-M.: Absolute UV absorption cross sections of dimethyl substituted Criegee intermediate $(\text{CH}_3)_2\text{COO}$, *Chem. Phys. Lett.*, 653, 155-160, <https://doi.org/10.1016/j.cplett.2016.04.082>, 2016.



- 250 Chao, W., Hsieh, J.-T., Chang, C.-H., and Lin, J. J.-M.: Direct kinetic measurement of the reaction of the simplest Criegee intermediate with water vapor, *Science*, 347, 751, <https://doi.org/10.1126/science.1261549>, 2015.
- Chao, W., Lin, Y.-H., Yin, C., Lin, W.-H., Takahashi, K., and Lin, J. J.-M.: Temperature and isotope effects in the reaction of CH_3CHOO with methanol, *Phys. Chem. Chem. Phys.*, 21, 13633-13640, <https://doi.org/10.1039/C9CP02534K>, 2019.
- Charlson, R. J., Lovelock, J. E., Andreae, M. O., and Warren, S. G.: Oceanic phytoplankton, atmospheric sulphur, cloud
255 albedo and climate, *Nature*, 328, 655-661, <https://doi.org/10.1038/326655a0>, 1987.
- Chen, Q., Sherwen, T., Evans, M., and Alexander, B.: DMS oxidation and sulfur aerosol formation in the marine troposphere: a focus on reactive halogen and multiphase chemistry, *Atmos. Chem. Phys.*, 18, 13617-13637, <https://doi.org/10.5194/acp-18-13617-2018>, 2018.
- Chhantyal-Pun, R., Davey, A., Shallcross, D. E., Percival, C. J., and Orr-Ewing, A. J.: A kinetic study of the CH_2OO Criegee
260 intermediate self-reaction, reaction with SO_2 and unimolecular reaction using cavity ring-down spectroscopy, *Phys. Chem. Chem. Phys.*, 17, 3617-3626, <https://doi.org/10.1039/C4CP04198D>, 2015.
- Chhantyal-Pun, R., Shannon, R. J., Tew, D. P., Caravan, R. L., Duchi, M., Wong, C., Ingham, A., Feldman, C., McGillen, M. R., Khan, M. A. H., Antonov, I. O., Rotavera, B., Ramasesha, K., Osborn, D. L., Taatjes, C. A., Percival, C. J., Shallcross, D. E., and Orr-Ewing, A. J.: Experimental and computational studies of Criegee intermediate reactions with NH_3 and
265 CH_3NH_2 , *Phys. Chem. Chem. Phys.*, 21, 14042-14052, <https://doi.org/10.1039/C8CP06810K>, 2019.
- Eskola, A. J., Wojcik-Pastuszka, D., Ratajczak, E., and Timonen, R. S.: Kinetics of the reactions of CH_2Br and CH_2I radicals with molecular oxygen at atmospheric temperatures, *Phys. Chem. Chem. Phys.*, 8, 1416-1424, <https://doi.org/10.1039/B516291B>, 2006.
- Faloona, I.: Sulfur processing in the marine atmospheric boundary layer: A review and critical assessment of modeling
270 uncertainties, *Atmos. Environ.*, 43, 2841-2854, <https://doi.org/10.1016/j.atmosenv.2009.02.043>, 2009.
- Foreman, E. S., Kapnas, K. M., and Murray, C.: Reactions between Criegee intermediates and the inorganic acids HCl and HNO_3 : kinetics and atmospheric implications, *Angew. Chem., Int. Ed.*, 55, 10419-10422, <https://doi.org/10.1002/anie.201604662>, 2016.
- Gutbrod, R., Kraka, E., Schindler, R. N., and Cremer, D.: Kinetic and theoretical investigation of the gas-phase ozonolysis of
275 isoprene: carbonyl oxides as an important source for OH radicals in the atmosphere, *J. Am. Chem. Soc.*, 119, 7330-7342, <https://doi.org/10.1021/ja970050c>, 1997.
- Hearn, C. H., Turcu, E., and Joens, J. A.: The near UV absorption spectra of dimethyl sulfide, diethyl sulfide and dimethyl disulfide at $T=300\text{ K}$, *Atmos. Environ., Part A*, 24, 1939-1944, [https://doi.org/10.1016/0960-1686\(90\)90527-T](https://doi.org/10.1016/0960-1686(90)90527-T), 1990.
- Huang, H.-L., Chao, W., and Lin, J. J.-M.: Kinetics of a Criegee intermediate that would survive high humidity and may
280 oxidize atmospheric SO_2 , *Proc. Natl. Acad. Sci.*, 112, 10857-10862, <https://doi.org/10.1073/pnas.1513149112> 2015.
- Jardine, K., Yañez-Serrano, A. M., Williams, J., Kunert, N., Jardine, A., Taylor, T., Abrell, L., Artaxo, P., Guenther, A., Hewitt, C. N., House, E., Florentino, A. P., Manzi, A., Higuchi, N., Kesselmeier, J., Behrendt, T., Veres, P. R., Derstroff,



- B., Fuentes, J. D., Martin, S. T., and Andreae, M. O.: Dimethyl sulfide in the Amazon rain forest, *Global Biogeochem. Cycles*, 29, 19-32, <https://doi.org/10.1002/2014GB004969>, 2015.
- 285 Johnson, D., and Marston, G.: The gas-phase ozonolysis of unsaturated volatile organic compounds in the troposphere, *Chem. Soc. Rev.*, 37, 699-716, <https://doi.org/10.1039/B704260B>, 2008.
- Khan, M. A. H., Percival, C. J., Caravan, R. L., Taatjes, C. A., and Shallcross, D. E.: Criegee intermediates and their impacts on the troposphere, *Environ. Sci.: Processes Impacts*, 20, 437-453, <https://doi.org/10.1039/C7EM00585G>, 2018.
- Kim, S., Guenther, A., Lefer, B., Flynn, J., Griffin, R., Rutter, A. P., Gong, L., and Cevik, B. K.: Potential role of stabilized
 290 Criegee radicals in sulfuric acid production in a high biogenic VOC environment, *Environ. Sci. Technol.*, 49, 3383-3391, <https://doi.org/10.1021/es505793t>, 2015.
- Lee, Y. P.: Perspective: Spectroscopy and kinetics of small gaseous Criegee intermediates, *J. Chem. Phys.*, 143, 020901, <https://doi.org/10.1063/1.4923165>, 2015.
- Lewis, T. R., Blitz, M. A., Heard, D. E., and Seakins, P. W.: Direct evidence for a substantive reaction between the Criegee
 295 intermediate, CH_2OO , and the water vapour dimer, *Phys. Chem. Chem. Phys.*, 17, 4859-4863, <https://doi.org/10.1039/C4CP04750H>, 2015.
- Li, Y.-L., Lin, Y.-H., Yin, C., Takahashi, K., Chiang, C.-Y., Chang, Y.-P., and Lin, J. J.-M.: Temperature-dependent rate coefficient for the reaction of CH_3SH with the simplest Criegee intermediate, *J. Phys. Chem. A*, 123, 4096-4103, <https://doi.org/10.1021/acs.jpca.8b12553>, 2019.
- 300 Li, Y.-L., Kuo, M.-T., and Lin, J. J.-M.: Unimolecular decomposition rates of a methyl-substituted Criegee intermediate syn- CH_3CHOO , *RSC Advances*, 10, 8518-8524, <https://doi.org/10.1039/D0RA01406K>, 2020.
- Limão-Vieira, P., Eden, S., Kendall, P. A., Mason, N. J., and Hoffmann, S. V.: High resolution VUV photo-absorption cross-section for dimethylsulphide, $(\text{CH}_3)_2\text{S}$, *Chem. Phys. Lett.*, 366, 343-349, [https://doi.org/10.1016/S0009-2614\(02\)01651-2](https://doi.org/10.1016/S0009-2614(02)01651-2), 2002.
- 305 Lin, H.-Y., Huang, Y.-H., Wang, X., Bowman, J. M., Nishimura, Y., Witek, H. A., and Lee, Y.-P.: Infrared identification of the Criegee intermediates syn- and anti- CH_3CHOO , and their distinct conformation-dependent reactivity, *Nat. Commun.*, 6, 7012, <https://doi.org/10.1038/ncomms8012>, 2015.
- Lin, J. J.-M., and Chao, W.: Structure-dependent reactivity of Criegee intermediates studied with spectroscopic methods, *Chem. Soc. Rev.*, 46, 7483-7497, <https://doi.org/10.1039/C7CS00336F>, 2017.
- 310 Lin, Y.-H., Li, Y.-L., Chao, W., Takahashi, K., and Lin, J. J.-M.: The role of the iodine-atom adduct in the synthesis and kinetics of methyl vinyl ketone oxide — a resonance-stabilized Criegee intermediate, submitted for publication in *Phys. Chem. Chem. Phys.*, 2020.
- Lin, Y.-H., Takahashi, K., and Lin, J. J.-M.: Reactivity of Criegee intermediates toward carbon dioxide, *J. Phys. Chem. Lett.*, 9, 184-188, <https://doi.org/10.1021/acs.jpcllett.7b03154>, 2018.
- 315 Liu, F., Beames, J. M., Green, A. M., and Lester, M. I.: UV spectroscopic characterization of dimethyl- and ethyl-substituted carbonyl oxides, *J. Phys. Chem. A*, 118, 2298-2306, <https://doi.org/10.1021/jp412726z>, 2014a.



- Liu, F., Beames, J. M., Petit, A. S., McCoy, A. B., and Lester, M. I.: Infrared-driven unimolecular reaction of CH_3CHOO Criegee intermediates to OH radical products, *Science*, 345, 1596-1598, <https://doi.org/10.1126/science.1257158>, 2014b.
- Liu, Y., Bayes, K. D., and Sander, S. P.: Measuring rate constants for reactions of the simplest Criegee intermediate (CH_2OO) by monitoring the OH radical, *J. Phys. Chem. A*, 118, 741-747, <https://doi.org/10.1021/jp407058b>, 2014c.
- McCarthy, M. C., Cheng, L., Crabtree, K. N., Martinez, O., Nguyen, T. L., Womack, C. C., and Stanton, J. F.: The simplest Criegee intermediate ($\text{H}_2\text{C}=\text{O}-\text{O}$): isotopic spectroscopy, equilibrium structure, and possible formation from atmospheric lightning, *J. Phys. Chem. Lett.*, 4, 4133-4139, <https://doi.org/10.1021/jz4023128>, 2013.
- Meidan, D., Holloway, J. S., Edwards, P. M., Dubé, W. P., Middlebrook, A. M., Liao, J., Welti, A., Graus, M., Warneke, C., Ryerson, T. B., Pollack, I. B., Brown, S. S., and Rudich, Y.: Role of Criegee intermediates in secondary sulfate aerosol formation in nocturnal power plant plumes in the southeast US, *ACS Earth Space Chem.*, 3, 748-759, <https://doi.org/10.1021/acsearthspacechem.8b00215>, 2019.
- Nakajima, M., Yue, Q., and Endo, Y.: Fourier-transform microwave spectroscopy of an alkyl substituted Criegee intermediate anti- CH_3CHOO , *J. Mol. Spectrosc.*, 310, 109-112, <https://doi.org/10.1016/j.jms.2014.11.004>, 2015.
- Newland, M. J., Rickard, A. R., Vereecken, L., Muñoz, A., Ródenas, M., and Bloss, W. J.: Atmospheric isoprene ozonolysis: impacts of stabilised Criegee intermediate reactions with SO_2 , H_2O and dimethyl sulfide, *Atmos. Chem. Phys.*, 15, 9521-9536, <https://doi.org/10.5194/acp-15-9521-2015>, 2015.
- Nguyen, T. B., Tyndall, G. S., Crounse, J. D., Teng, A. P., Bates, K. H., Schwantes, R. H., Coggon, M. M., Zhang, L., Feiner, P., Milller, D. O., Skog, K. M., Rivera-Rios, J. C., Dorris, M., Olson, K. F., Koss, A., Wild, R. J., Brown, S. S., Goldstein, A. H., de Gouw, J. A., Brune, W. H., Keutsch, F. N., Seinfeld, J. H., and Wennberg, P. O.: Atmospheric fates of Criegee intermediates in the ozonolysis of isoprene, *Phys. Chem. Chem. Phys.*, 18, 10241-10254, <https://doi.org/10.1039/C6CP00053C>, 2016.
- Novelli, A., Vereecken, L., Lelieveld, J., and Harder, H.: Direct observation of OH formation from stabilised Criegee intermediates, *Phys. Chem. Chem. Phys.*, 16, 19941-19951, <https://doi.org/10.1039/C4CP02719A>, 2014.
- Novelli, A., Hens, K., Tatum Ernest, C., Martinez, M., Nölscher, A. C., Sinha, V., Paasonen, P., Petäjä, T., Sipilä, M., Elste, T., Plass-Dülmer, C., Phillips, G. J., Kubistin, D., Williams, J., Vereecken, L., Lelieveld, J., and Harder, H.: Estimating the atmospheric concentration of Criegee intermediates and their possible interference in a FAGE-LIF instrument, *Atmos. Chem. Phys.*, 17, 7807-7826, <https://doi.org/10.5194/acp-17-7807-2017>, 2017.
- Osborn, D. L., and Taatjes, C. A.: The physical chemistry of Criegee intermediates in the gas phase, *Int. Rev. Phys. Chem.*, 34, 309-360, <https://doi.org/10.1080/0144235X.2015.1055676>, 2015.
- Percival, C. J., Welz, O., Eskola, A. J., Savee, J. D., Osborn, D. L., Topping, D. O., Lowe, D., Utembe, S. R., Bacak, A., McFiggans, G., Cooke, M. C., Xiao, P., Archibald, A. T., Jenkin, M. E., Derwent, R. G., Riipinen, I., Mok, D. W. K., Lee, E. P. F., Dyke, J. M., Taatjes, C. A., and Shallcross, D. E.: Regional and global impacts of Criegee intermediates on atmospheric sulphuric acid concentrations and first steps of aerosol formation, *Faraday Discuss.*, 165, 45-73, <https://doi.org/10.1039/C3FD00048F>, 2013.



- Sander, S. P., Abbatt, J., Barker, J. R., Burkholder, J. B., Friedl, R. R., Golden, D. M., Huie, R. E., Kolb, C. E., Kurylo, M. J., Moortgat, G. K., Orkin, V. L., and Wine, P. H.: Chemical kinetics and photochemical data for use in atmospheric studies, Evaluation Number 17, JPL Publication 10-6, Jet Propulsion Laboratory, Pasadena, <http://jpldataeval.jpl.nasa.gov/>, 2011.
- Sheps, L.: Absolute ultraviolet absorption spectrum of a Criegee intermediate CH_2OO , *J. Phys. Chem. Lett.*, 4, 4201-4205, <https://doi.org/10.1021/jz402191w>, 2013.
- Smith, M. C., Ting, W.-L., Chang, C.-H., Takahashi, K., Boering, K. A., and Lin, J. J.-M.: UV absorption spectrum of the C2 Criegee intermediate CH_3CHOO , *J. Chem. Phys.*, 141, 074302, <https://doi.org/10.1063/1.4892582>, 2014.
- Smith, M. C., Chao, W., Takahashi, K., Boering, K. A., and Lin, J. J.-M.: Unimolecular decomposition rate of the Criegee intermediate $(\text{CH}_3)_2\text{COO}$ measured directly with UV absorption spectroscopy, *J. Phys. Chem. A*, 120, 4789-4798, <https://doi.org/10.1021/acs.jpca.5b12124>, 2016.
- Stephenson, T. A., and Lester, M. I.: Unimolecular decay dynamics of Criegee intermediates: energy-resolved rates, thermal rates, and their atmospheric impact, *Int. Rev. Phys. Chem.*, 39, 1-33, <https://doi.org/10.1080/0144235X.2020.1688530>, 2020.
- Stone, D., Blitz, M., Daubney, L., Howes, N. U. M., and Seakins, P. W.: Kinetics of CH_2OO reactions with SO_2 , NO_2 , NO , H_2O and CH_3CHO as a function of pressure, *Phys. Chem. Chem. Phys.*, 16, 1139-1149, <https://doi.org/10.1039/C3CP54391A>, 2014.
- Su, M.-N., and Lin, J. J.-M.: Note: A transient absorption spectrometer using an ultra bright laser-driven light source, *Rev. Sci. Instrum.*, 84, 086106, <https://doi.org/10.1063/1.4818977>, 2013.
- Su, Y.-T., Huang, Y.-H., Witek, H. A., and Lee, Y.-P.: Infrared absorption spectrum of the simplest Criegee intermediate CH_2OO , *Science*, 340, 174-176, <https://doi.org/10.1126/science.1234369>, 2013.
- Taatjes, C. A., Welz, O., Eskola, A. J., Savee, J. D., Osborn, D. L., Lee, E. P. F., Dyke, J. M., Mok, D. W. K., Shallcross, D. E., and Percival, C. J.: Direct measurement of Criegee intermediate (CH_2OO) reactions with acetone, acetaldehyde, and hexafluoroacetone, *Phys. Chem. Chem. Phys.*, 14, 10391-10400, <https://doi.org/10.1039/C2CP40294G>, 2012.
- Taatjes, C. A., Welz, O., Eskola, A. J., Savee, J. D., Scheer, A. M., Shallcross, D. E., Rotavera, B., Lee, E. P. F., Dyke, J. M., Mok, D. K. W., Osborn, D. L., and Percival, C. J.: Direct measurements of conformer-dependent reactivity of the Criegee intermediate CH_3CHOO , *Science*, 340, 177-180, <https://doi.org/10.1126/science.1234689>, 2013.
- Ting, W.-L., Chen, Y.-H., Chao, W., Smith, M. C., and Lin, J. J.-M.: The UV absorption spectrum of the simplest Criegee intermediate CH_2OO , *Phys. Chem. Chem. Phys.*, 16, 10438-10443, <https://doi.org/10.1039/C4CP00877D>, 2014.
- Vansco, M. F., Marchetti, B., and Lester, M. I.: Electronic spectroscopy of methyl vinyl ketone oxide: a four-carbon unsaturated Criegee intermediate from isoprene ozonolysis, *J. Chem. Phys.*, 149, 244309, <https://doi.org/10.1063/1.5064716>, 2018.
- Vansco, M. F., Marchetti, B., Trongsiwat, N., Bhagde, T., Wang, G., Walsh, P. J., Klippenstein, S. J., and Lester, M. I.: Synthesis, electronic spectroscopy, and photochemistry of methacrolein oxide: a four-carbon unsaturated Criegee



- intermediate from isoprene ozonolysis, *J. Am. Chem. Soc.*, 141, 15058-15069, <https://doi.org/10.1021/jacs.9b05193>,
385 2019.
- Vereecken, L., Novelli, A., and Taraborrelli, D.: Unimolecular decay strongly limits the atmospheric impact of Criegee intermediates, *Phys. Chem. Chem. Phys.*, 19, 31599-31612, <https://doi.org/10.1039/C7CP05541B>, 2017.
- Wang, M. Y., Yao, L., Zheng, J., Wang, X., Chen, J. M., Yang, X., Worsnop, D. R., Donahue, N. M., and Wang, L.: Reactions of atmospheric particulate stabilized Criegee intermediates lead to high-molecular-weight aerosol components, 390 *Environ. Sci. Technol.*, 50, 5702-5710, <https://doi.org/10.1021/acs.est.6b02114>, 2016.
- Welz, O., Savee, J. D., Osborn, D. L., Vasu, S. S., J., P. C., Shallcross, D. E., and Taatjes, C. A.: Direct kinetic measurements of Criegee intermediate CH_2OO formed by reaction of CH_2I with O_2 , *Science*, 335, 204-204, <https://doi.org/10.1126/science.1213229>, 2012.
- Welz, O., Eskola, A. J., Sheps, L., Rotavera, B., Savee, J. D., Scheer, A. M., Osborn, D. L., Lowe, D., Murray B., A., Xiao, 395 P., Khan, M. A. H., Percival, C. J., Shallcross, D. E., and Taatjes, C. A.: Rate coefficients of C1 and C2 Criegee intermediate reactions with formic and acetic acid near the collision limit: direct kinetics measurements and atmospheric implications, *Angew. Chem., Int. Ed.*, 53, 4547-4550, <https://doi.org/10.1002/anie.201400964>, 2014.
- Yvon, S. A., Saltzman, E. S., Cooper, D. J., Bates, T. S., and Thompson, A. M.: Atmospheric sulfur cycling in the tropical Pacific marine boundary layer (12°S , 135°W): a comparison of field data and model results: 1. dimethylsulfide, *J. Geophys. Res.: Atmos.*, 101, 6899-6909, <https://doi.org/10.1029/95JD03356>, 1996.
400
- Zhang, D., Lei, W., and Zhang, R.: Mechanism of OH formation from ozonolysis of isoprene: kinetics and product yield, *Chem. Phys. Lett.*, 358, 171-179, [https://doi.org/10.1016/S0009-2614\(02\)00260-9](https://doi.org/10.1016/S0009-2614(02)00260-9), 2002.
- Zhou, X., Liu, Y., Dong, W., and Yang, X.: Unimolecular reaction rate measurement of syn- CH_3CHOO , *J. Phys. Chem. Lett.*, 10, 4817-4821, <https://doi.org/10.1021/acs.jpcclett.9b01740>, 2019.
405

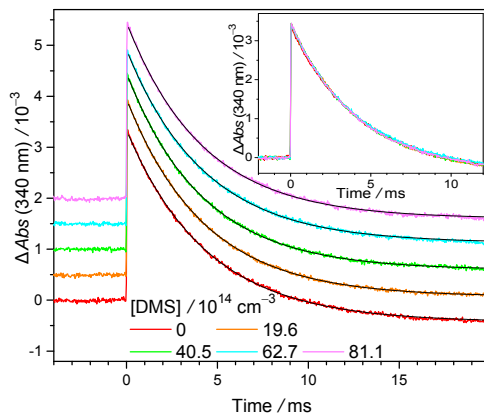


Figure 1: Representative time traces of CH_2OO absorption recorded at 340 ± 5 nm under various $[\text{DMS}]$. The traces are shifted upward by various amounts for clearer visualization. Smooth black lines are the exponential fit. The photolysis laser (308 nm) pulse defines $t = 0$. The negative baseline (more obvious at long reaction time) is due to depletion of the precursor, CH_2I_2 , which absorbs weakly at 340 nm ($\sigma = 8.33 \times 10^{-19} \text{ cm}^2$). (Atkinson et al., 2008) This depletion is constant in the probed time window and would not affect the kinetics of CH_2OO . Inset: The profiles without upshifting to show the overlapping. See Exp#1 of Table S1 for detailed experimental conditions.

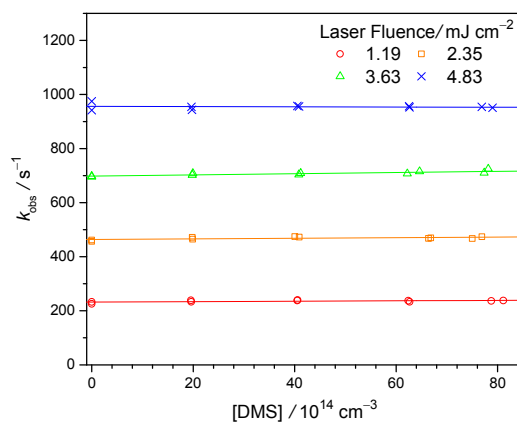


Figure 2: k_{obs} against $[\text{DMS}]$ determined from experiments (Exp#1-4, Table S1) at different photolysis laser fluences $I_{308\text{nm}}$; solid lines are linear fits.

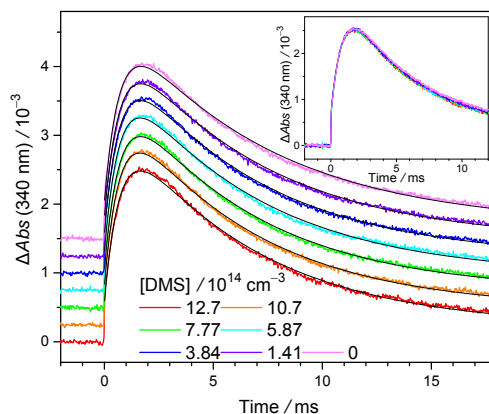


Figure 3: Representative MVKO absorbance-time profiles recorded at 340 nm under various [DMS] (298 K, 300 Torr, see Exp#16 of Table S3). The profiles are upshifted by various amounts to avoid overlapping. The color lines are experimental data and the smooth black lines are the model fit. Inset: The profiles without upshifting to show the overlapping.

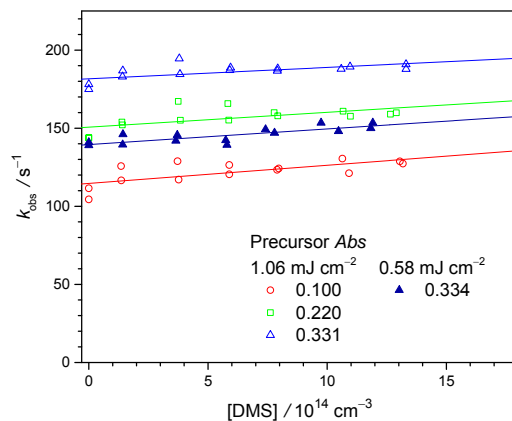


Figure 4: Plot of the observed decay rate coefficient of MVKO k_{obs} against [DMS] at various laser fluences and precursor absorbances (Exp#15–18). For each data point, the fitting error bar is less than 1% (thus, not shown).



425 Table 1: Summary of the bimolecular reaction rate coefficients of $\text{Cl}+\text{SO}_2$ and $\text{Cl}+\text{DMS}$.

| Cl | k_{DMS} / $\text{cm}^3 \text{s}^{-1}$ | k_{SO_2} / $\text{cm}^3 \text{s}^{-1}$ | $k_{\text{DMS}} / k_{\text{SO}_2}$ | Reference |
|------------------------|---|--|------------------------------------|---------------------|
| CH_2OO | $\leq 4.2 \times 10^{-15}$ | $3.7 \times 10^{-11, a}$ | $< 1.1 \times 10^{-4}$ | This work |
| MVKO | $\leq 1.6 \times 10^{-14}$ | $4.1 \times 10^{-11, b}$ | $< 3.9 \times 10^{-4}$ | This work |
| ClIs | - | - | 3.5 ± 1.8 | Newland et al. 2015 |

^a The average value of $(3.4 \pm 0.4) \times 10^{-11}$ (Stone et al., 2014), $(3.5 \pm 0.3) \times 10^{-11}$ (Liu et al., 2014c), $(3.8 \pm 0.04) \times 10^{-11}$ (Chhantyal-Pun et al., 2015), $(3.9 \pm 0.7) \times 10^{-11}$ (Welz et al., 2012), and $(4.1 \pm 0.3) \times 10^{-11}$ (Sheps, 2013).

^b Caravan et al. 2020.